

ASTROMETRIC MEASUREMENTS OF SATELLITES WITH DYNAMIC VISION SENSOR

Michał Żolnowski⁽¹⁾, Krzysztof Kamiński⁽²⁾, Tobias Delbruck⁽³⁾, Alicja Gąsiorowska⁽²⁾, Justyna Gołębiowska⁽²⁾, Marcin Gędek⁽¹⁾, Monika Kamińska⁽²⁾, Joachim Kruger⁽²⁾⁽⁴⁾, Mikołaj Krużyński⁽²⁾, Mikołaj Pieniowski⁽¹⁾, Rafał Reszelewski⁽¹⁾, Krzysztof Romanowski⁽⁴⁾, Edwin Wnuk⁽²⁾, Wojciech Dimitrow⁽²⁾, Wojciech Mich⁽⁴⁾

⁽¹⁾6ROADS Sp z o.o., Godebskiego Street 55a, Kraków, Poland, michal.zolnowski@6roads.com.pl

⁽²⁾Astronomical Observatory Institute, Faculty of Physics, Adam Mickiewicz University, Poznań, Poland, chrisk@amu.edu.pl

⁽³⁾Sensors Group, Institute of Neuroinformatics, UZH-ETH Zurich, Winterthurerstr. 190, CH-8057 Zurich, tobi@ini.uzh.ch

⁽⁴⁾ITTI Sp z o.o., Rubież 46, Poznań, Poland

ABSTRACT

The Dynamic Vision Sensor (DVS) technology, which could potentially be utilized in various SST activities, has been the subject of our research over the last several months. This type of camera records from each pixel an asynchronous stream of events of brightness variation changes, rather than integrated intensity recorded simultaneously over selected exposure time. Due to its novel approach to visual data retrieving and processing, DVS needs evaluation as a potential tool in the SST domain. Several observing methods have been proposed and tested. The key parameters considered in our studies are the camera's timing accuracy and astrometric precision. The paper presents the results of the world's first astrometric measurements of satellites observed with a DVS camera performed on a GNSS satellite. Furthermore, a series of observations of principally GEO and MEO, but also LEO, targets was conducted. Satellites were observed with a few different optical telescopes to evaluate DVS camera's performance in different configurations. A whole observing methodology and reduction pipeline has been developed, including dedicated GNSS clock for event timestamping and dedicated software capable of converting DVS data stream from native AEDAT format to a series of FITS images.

1 INTRODUCTION

Dynamic Vision Sensor technology has been suggested as an interesting alternative to CCD and CMOS cameras several years ago (see [1] or [4]). Its primary advantage has been pointed out as a huge dynamic range allowing for daytime detections. Also the principle of operation of DVA cameras seems to fit perfectly for satellite survey observations, with its low latency and sparse low data rate. On the other hand the DVS technology is relatively new, prototypical, uncooled and lacks large high-

sensitivity sensors with fully employed capabilities for low light applications. In this project we decided to use a first back-side illumination hybrid DVS and imaging camera prototype, namely DAVIS 346BSI developed by University of Zurich.

2 DVS SPECIFICATIONS

The DVS camera, which underwent thorough examination was DAVIS 346BSI. The pixel size of this camera is $18.5\mu\text{m} \times 18.5\mu\text{m}$, the array size of $6.4\text{mm} \times 4.8\text{mm}$, 100% fill factor and the peak quantum efficiency of 93%. Three copies of the camera were assembled for the tests. Fig.1 presents the DAVIS 346BSI camera.



Figure 1. DAVIS 346BSI camera.

3 HARDWARE & SOFTWARE PREPARATION

By default, the camera's firmware timestamps each recorded event with microsecond resolution using its internal oscillator without reference to any external source. The beginning of each recording (event stream) is time-stamped with PC control software (jaerViewer)

which can be referenced to UTC via NTP with a typical accuracy at the level of 10 milliseconds. LEO tracking requires accuracy at the level of sub-milliseconds and millisecond accuracy is required for higher orbits. In order to meet those accuracy requirements and to provide the time reference independent from Internet connection delays, external time impulses are injected into the DAVIS 346BSI camera in periodic manner. A dedicated GNSS based clock has been constructed to generate these impulses with microsecond accuracy. They are recorded by DAVIS 346BSI camera as so called “special” events, which are time-stamped in the same way as normal events, however they can be easily distinguished. Two time measurements of the same impulse, one by GNSS clock, one by DAVIS 346BSI camera timestamp enable the conversion of the camera’s internal clock to the UTC time scale. Fig.2 presents the scheme of DAVIS 346BSI camera events timing system.

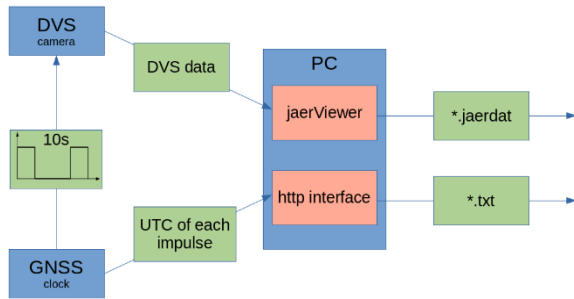


Figure 2. DAVIS 346BSI camera events timing system.

Subsequently, it was necessary to develop software, which would enable the effective use of the data provided by the DAVIS 346BSI cameras with a regular astronomical reduction and analysis pipelines. The software – AEDAT Converter – performs two tasks simultaneously. First – it transforms event data stream from AEDAT format to FITS images by counting all events in each pixel between selected start and stop time and saving them as integer ADUs. User is able to select single or multiple time segments and event types to be saved. The second functionality is to linearly interpolate time passage between recorded “special” events and convert internal DVS timestamps into UTC for each event individually. Overall this software allows to select into how many images each recording is converted and therefore it controls the timing resolution of resulting image series up to 1 microsecond, which is the limit of DVS timestamps precision. Fig. 3 presents the scheme of the process of converting timestamps to UTC.

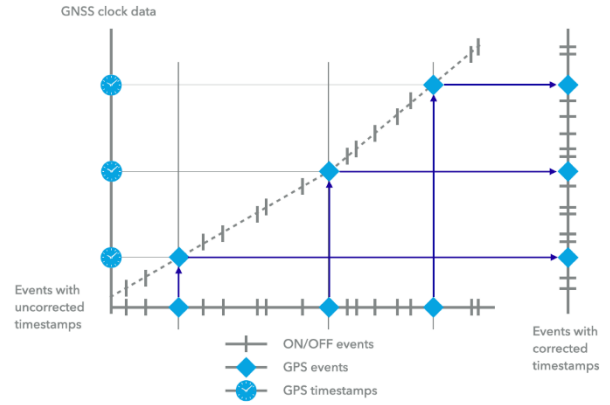


Figure 3. Conversion of timestamps to UTC

4 LABORATORY ANALYSIS

A series of laboratory test with artificial, moving light sources were conducted prior to observations in order to determine a set of optimum DVS camera settings. Two teams using different approaches found a slightly different combination of settings that were later used during observations. The results are presented in Tab.1

Parameter	Default settings	6Roads Night	6Roads Daylight	AO AMU Night	AO AMU Daylight
DiffBn	5.1n	115.5n	31.7n	51.7n	51.7n
OnBn	194.5n	317.6n	95.7n	244.6n	486.3n
OffBn	124.6p	0	0	97.9p	49.3p
PrBp	7.9p	6.4p	6.0p	7.9p	7.9p
PrSFBp	8.0p	4.6p	4.3p	8.0p	8.0p
RefrBp	593.6p	5.6n	5.1n	593.6p	593.6p

Table 1. DAVIS 346BSI camera settings used during the night-time and daytime observations.

In order to better understand DVS camera behaviour in low light observations a simple test was conducted to measure the level of delays of two simultaneous light-source blinks. Using our DAVIS 346BSI camera equipped with a GNSS clock we recorded blinks of a LED, controlled with another GPS receiver in order to compare the actual time of LED light up with the recorded time. Additionally, by observing also a LED reflection from a piece of glass we had the opportunity to compare reaction time at about 25x lower illumination, as illustrated in Fig. 4.

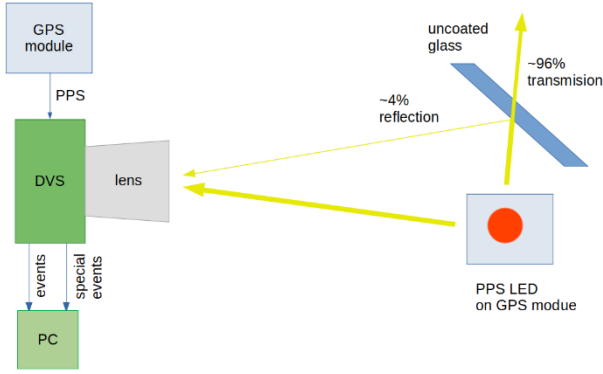


Figure 4. Testing setup for timing of a blinking LED experiment.

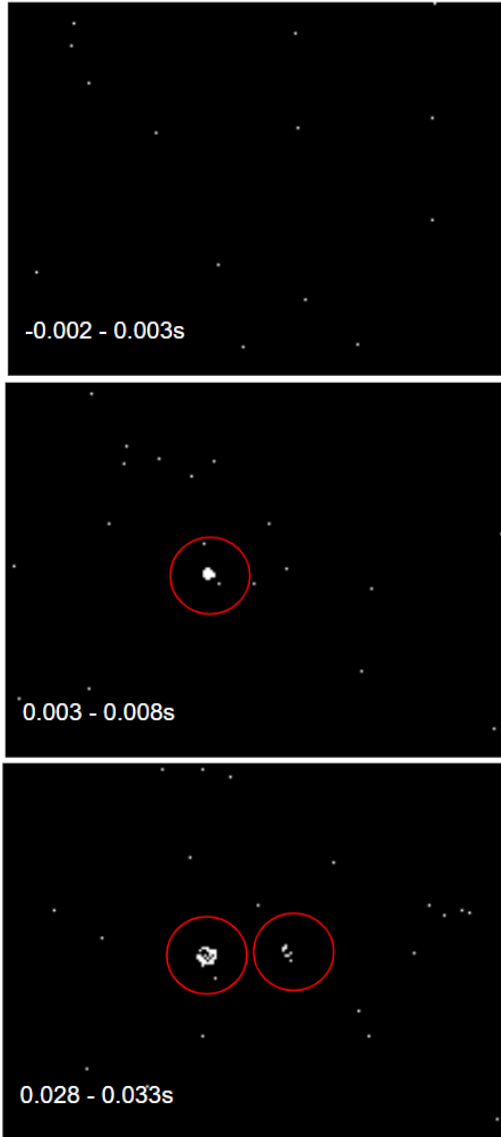


Figure 5. DAVIS 346BSI camera recording of a blinking LED and its reflection at three time intervals. In the top image no events are recorded even though a new second has started. In the middle image first events from

blighter light source is detected, but no events from its reflection. In the bottom image the dimmer light source blink is finally detected.

DVS setup	Bright source (direct LED)	Dim source (reflected LED)
Nighttime	$0.0029s \pm 0.0006s$	$0.015s \pm 0.003s$
Updated nighttime On Bias 1.32x higher	$0.0046s \pm 0.0014s$	$0.020s \pm 0.005s$
Daytime On Bias 2.27x lower	$0.0034s \pm 0.0006s$	$0.017s \pm 0.004s$

Table 2. DAVIS 346BSI delays in recording blinking LED and its 25x dimmer reflection.

As presented in Fig. 5 and Tab. 2 we detected measurable delays in all recordings, but the 25x dimmer light-source had a significantly larger delay. This result shows that DVS camera time bias is mostly negligible in case of GEO satellites observations, but significant in low orbit targets. It also shows that DVS camera can have different time bias for simultaneously observed objects if their brightness differs significantly, which can be difficult to correct for during analysis.

5 DVS OBSERVING METHODOLOGY

In both satellite survey and tracking observations, the DAVIS 346BSI camera struggles to detect stationary objects with 0.3m telescope — unless their magnitude is brighter than about 8. New observing techniques were developed in order to overcome this limitation.

5.1 Rotating shutter

The fundamental rule of the observations performed with the use of an event based sensor is the need for changes in the field of view. Tracked objects, such as stars or satellites do trigger events only because of scintillation or tracking errors, thus they have low SNR when compared to objects that move.

The initial solution devised by the project's members was employing a regular astronomical focuser in order to make stellar images out of focus and then rapidly focus them. Rapid refocusing would create an effect similar to reappearance of all objects in the field of view. However, this method proved to be inefficient.

Further tests consisted of quick covering and uncovering the end of the scope, which was aimed towards the sky. The dramatic increase in flux from zero, when the scope was covered, to full aperture when it was opened,

triggered a clearly visible cascade of star-caused events. Eventually, a commercial, 5-positional colour filter wheel produced by ASI ZWO was modified to periodically cover and evenly uncover the DAVIS' chip. Subsequently, it was installed between the camera and the telescope.

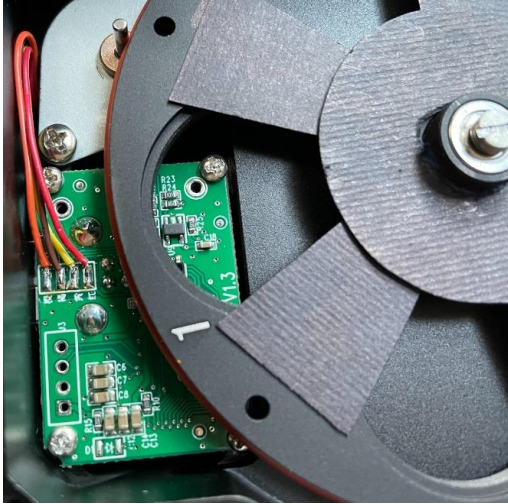


Figure 6. The modified CFW prior to attachment to the camera with modified blades of the shutter.

The filter wheel was modified to spin continuously at a user-selectable rate using an Arduino board. During observations, the filter acts as a rotating shutter, similarly to the shutters used with meteor cameras. Although the initial results of using this method were promising, it was noted that better darkening of the shutter's interior was necessary as stray light worsened the overall performance significantly. Therefore, entire interior of the wheel's chamber as well as the connector were covered with black material, resulting in improved results.

In further stages of the evaluation of the rotating shutter method it was revealed that it improves limiting magnitude for stationary objects to a large extent, however, not exactly to the same level as telescope movement. The test was performed when the Moon was full, thus the bright background could have had a negative impact on the results, which is worth noting.

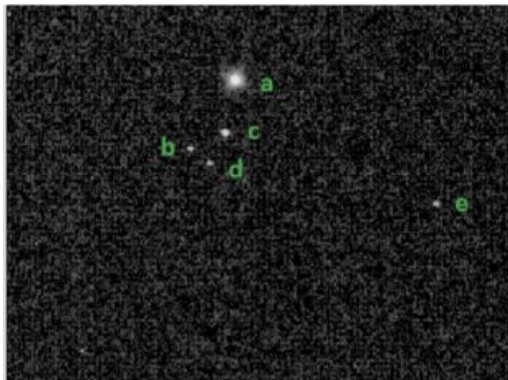


Figure 7. Observations of Alcyone star region in Pleiades with shutter method. The events triggered just after the blade of the shutter-like wheel has uncovered the DAVIS surface. The brightness of stars: (a) 2.85^m, (b) 8.52^m, (c) 6.29^m, (d) 8.97^m, (e) 8.71^m.

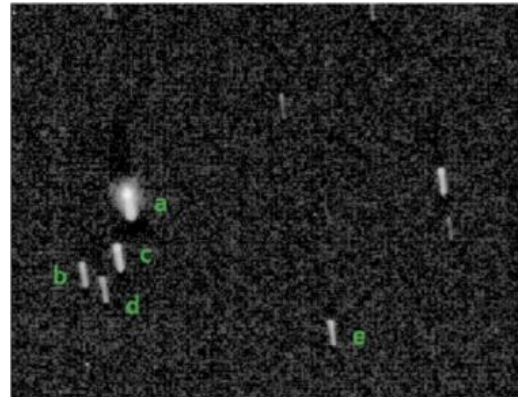


Figure 8. Observations of Alcyone star region in Pleiades during slewing of the mount with angular velocity of 240 arcsec/sec. Visible waves of ON and afterward OFF events generated by the movement toward the lower-right corner. The brightness of stars: (a) 2.85^m, (b) 8.52^m, (c) 6.29^m, (d) 8.97^m, (e) 8.71^m.

5.2 Epicyle tracking

Typically, satellite tracking is based directly on its ephemeris. When the ephemeris is sufficiently accurate and the telescope equatorial mount is accurate enough, the target satellite is kept constantly at the same camera pixels. In tracking with DVS camera this significantly reduced (by about 3-4 mag) the limiting magnitude and thus a different approach has been developed.

The satellite ephemeris was augmented with a circular motion, with the period of 6 seconds and the radius ranging from 6 to 15 arcseconds. As a result, the telescope was constantly wobbling around the ephemeris position of the satellite and satellite image was moving in the field of view with constant velocity. By manipulating the radius and period it was possible to determine at what angular speed the satellite was going to be moving during tracking. It was found that the best results can be obtained when the radius is 6 arcsec and the angular speed of the satellite is about 6 arcsec/sec.

The drawback to this method is the fact that it introduces complex, wave-like trails for reference stars, instead of simple, linearly elongated images. However, this issue can be solved by using a relatively long rotation period dividing the data into time steps small enough for the curvature of the stellar trails to become undetectable. Moreover, the AO AMU's astrometric software is capable of processing targets of any shape.

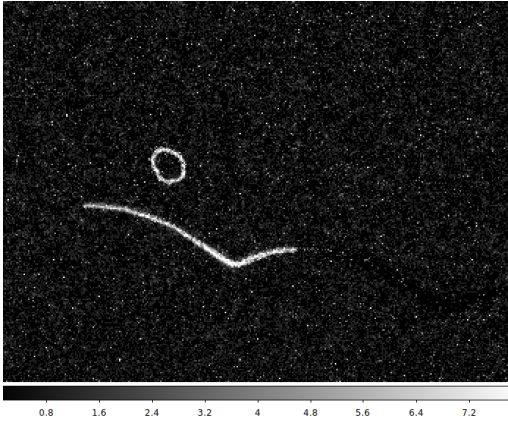


Figure 9. An example of “epicycle tracking” with a radius of 15 arcsec. This image shows “on” events registered while tracking GPS satellite no 45854. The telescope is tracking in such a way that the satellite is making small circles (slightly deformed because of $\cos(\text{Dec})$ and telescope inertia). A single star passing through the field of view is also visible.

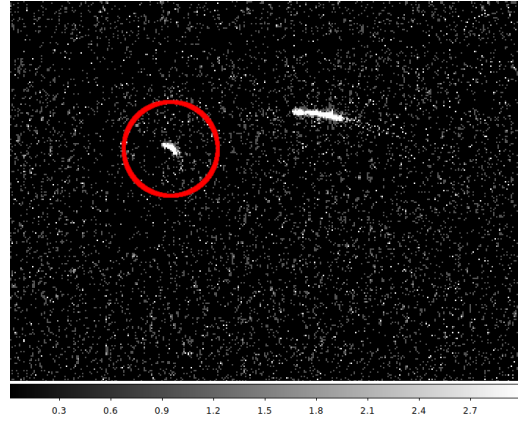
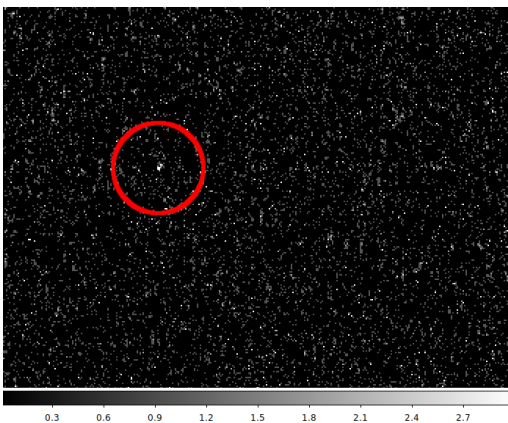
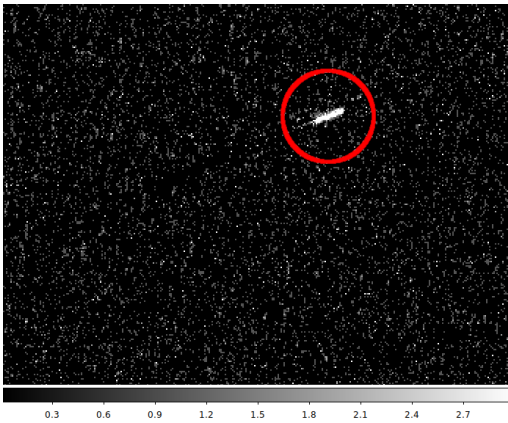


Figure 10. A comparison of the same satellite observations made at the same time with DAVIS 346BSI camera using different tracking modes. All images represent On events recorded during 1 sec. In the top image a satellite survey observation with a telescope in sidereal tracking mode is presented. A GPS satellite traveling at about 45 arcsec/sec is clearly visible. In the middle image a satellite tracking observation is presented. The satellite is only barely detectable and only in some images (one of the best is presented here). In the bottom image an “epicycle tracking” mode is presented. The satellite is clearly visible, at the level comparable with survey mode. Also a field star is recorded.



6 OBSERVATIONAL TESTS

6.1 GPS satellite tracking

In order to comprehensively compare DVS and sCMOS camera performance in satellite tracking a dedicated observation campaign was conducted between January and March 2021. The observations were conducted using two identical 12.5 inch f/8 telescopes. One of the telescopes was equipped with a DAVIS 346BSI camera. The other telescope was equipped with Andor Zyla 5.5 camera. Both cameras were connected with dedicated GNSS clocks for accurate image timing.

The software used for astrometry required at least 4 reference stars for a reliable solution. However, due to the narrow field of view of the DAVIS 346BSI camera as well as the satellite magnitudes rarely high enough for detection even when moving in the field of view, it was nearly impossible to meet this requirement using regular satellite tracking. As a result, the two novel techniques developed by 6ROADS and AO AMU, described in Section 5, were employed, as well as numerous small incremental improvements in reduction and analysis software.

On the 3rd of March 2021, the most successful observations were conducted. The observed target was a

GPS satellite (NORAD 40294, COSPAR 2014-068A). The telescope equipped with the DAVIS 346BSI camera collected events from 22:33:45 to 22:54:57 UTC. The data stream was converted to 2472 FITS images, each containing the “on” events solely and covering the timespan of 0.5s.

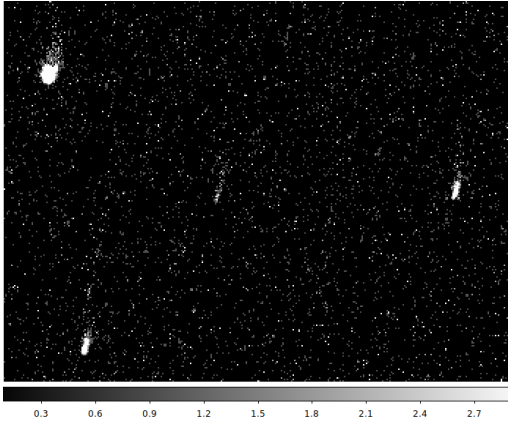


Figure 11. An example of GPS satellite tracking observation with DAVIS 346BSI camera and CDK12.5 f/8 telescope. The image is composed of “on” events recorded during 0.5 seconds. The satellite is not clearly visible here.

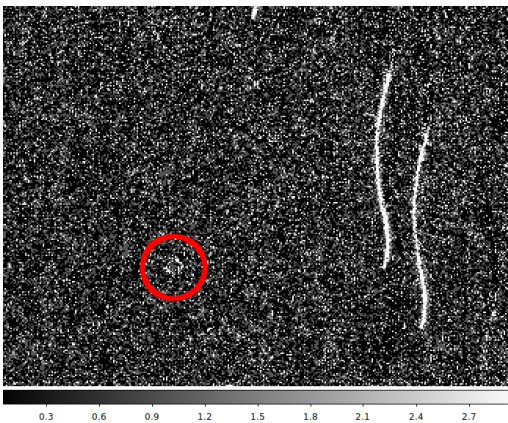


Figure 12. An example of GPS (40294) satellite tracking observation with DAVIS 346BSI camera and CDK12.5 f/8 telescope. The image is composed of “on” events recorded during 6.0 seconds. This is presented only to show where the satellite was observed (inside the red circle). The telescope epicycle tracking with the satellite constantly making small ($R=6$ arcsec) circles is visible.

The converted data was then analysed with Poznań Satellite Software Tools. Astrometric data were automatically extracted from 8 FITS files obtained from DAVIS 346BSI and from 992 FITS files obtained from Andor Zyla. The difference reflects the significantly smaller field of view of the DAVIS 346BSI camera and approximately 2 mag worse limiting magnitude. Rarely more than 3 stars with SNR higher than 2 were observed simultaneously for the software to identify the observed

field. Fig.14 presents the comparison of selected astrometric positions derived using DAVIS 346BSI and Zyla cameras.

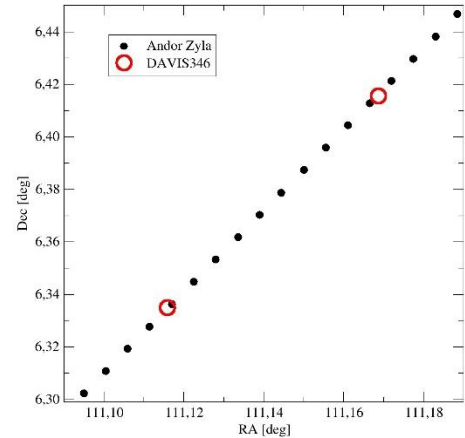


Figure 13. Comparison of selected astrometric position of GPS (40294) satellite derived on 08-03-2021 using DAVIS 346BSI and Zyla cameras.

All astrometric positions derived with both cameras were compared with high accuracy SP3 ephemeris provided by the GNSS operator. In order to derive the both regular and random shifts in RA and Dec, the differences were analysed statistically. Moreover, the difference along and across satellite orbits was calculated in order to have a better understanding of the nature of observed inaccuracies. The systematic differences along orbit were associated primarily with image or event timing systematic errors and the random differences across orbit were associated with overall astrometric accuracy. Large systematic differences across the satellite's orbit should not be observed unless there is an error in data reduction or in ephemeris. Small differences might be present due to, for example, noncentral target placement in images or systematic asymmetries in stellar images due to imperfect collimation, filed rotation etc.

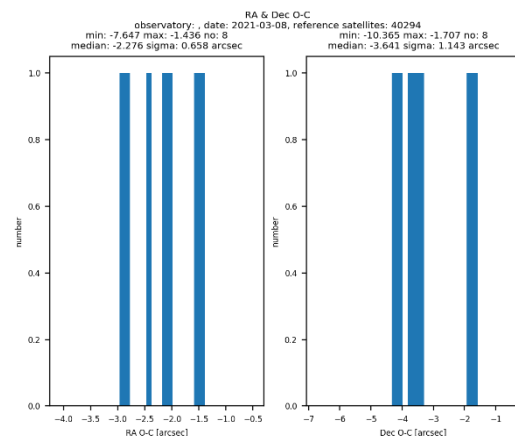


Figure 14. Distribution of errors in RA and Dec for GPS (40294) satellite observed with DAVIS 346BSI

camera.

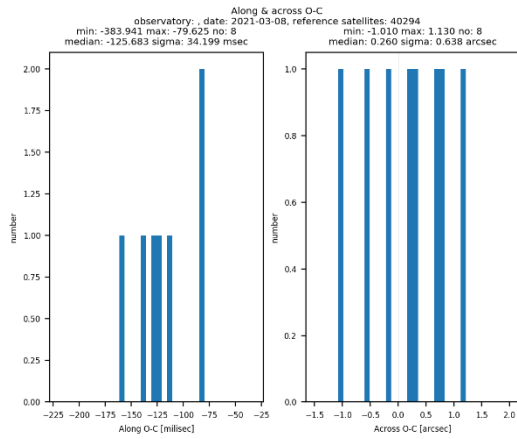


Figure 15. Distribution of errors along and across the trajectory of a GPS (40294) satellite observed with DAVIS 346BSI camera.

As seen in Fig.15, the data obtained using DAVIS contains small but systematic deviations from ephemeris positions. In the direction across satellite trajectory (Fig. 16) it can be noticed that the astrometric uncertainty is at the level of 0.6 arcsec, which can be considered a very good result. Moreover, no significant systematic deviation across orbit can be noticed. All of the systematic errors are oriented along the trajectory of the satellite, which indicates that they are most likely connected with event timing errors. Almost all of the measured points are concentrated around -125 ms time bias. With the satellite's angular velocity of about 40 arcsec/sec this corresponds to a shift of 5 arcsec or about 3 pixels in DAVIS camera. Several potential primary explanations of this shift have been considered.

According to the first one, the shift could be attributed to the slow reaction time of the DAVIS camera for very dim targets, such as the observed satellite. This effect was measured before in laboratory experiments and expected to produce a time shift at the level of about 20ms for target that were brighter than the satellite. Since the camera reaction time drops with target brightness it can be suspected that in case of nearly undetectable light source the delay will be significantly larger. This effect affects also all reference stars and creates flux dependent distortions in relative X,Y positions of stars and satellites. Another factor, which could potentially have an impact on the shift is the asymmetry of the images of reference stars. Each of the recorded moving object contains a clearly visible “comet tail”, produced by pixels, which trigger “on” events with significantly longer than usual delays. It seems that pixel triggering has the effect of increasing the probability of producing random events of the same polarity immediately afterwards. The asymmetry was partially mitigated by including higher weights to pixels with more events but we suspect that some residuals might still influence the results. It is hard

to estimate the order of magnitude of this effect, however if we assume that it can shift image by 1 to 2 pixels than it is slightly too low to explain the -125ms time bias. The final hypothesis was that the DAVIS 346BSI camera has an intrinsic time bias, which is considered probable as most cameras used in satellite tracking exhibit time bias at the level of tens or hundreds of milliseconds. It was noticed multiple times that the camera control software displayed a warning saying that “a non monotonic even has been detected” continuously throughout the observations. This could indicate that there were certain timing issues related to the camera’s firmware and hardware.

Similar analysis was performed for the images of the same satellite obtained simultaneously using the Andor Zyla camera on an identical telescope. Its result shows a time bias of -18 ms and astrometric uncertainty at the level of 0.15 arcsec (see Fig. 17 and 18).

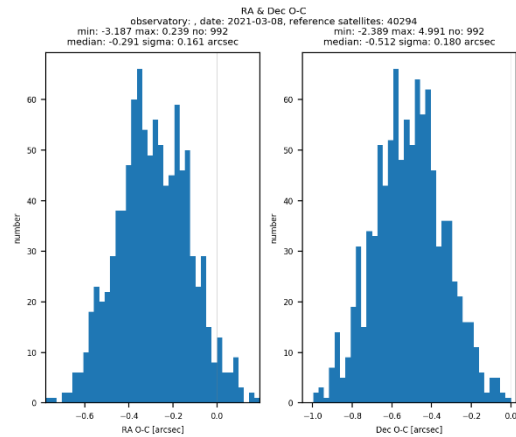


Figure 16. Distribution of errors in RA and Dec for GPS satellite observed with Andor Zyla 5.5 camera.

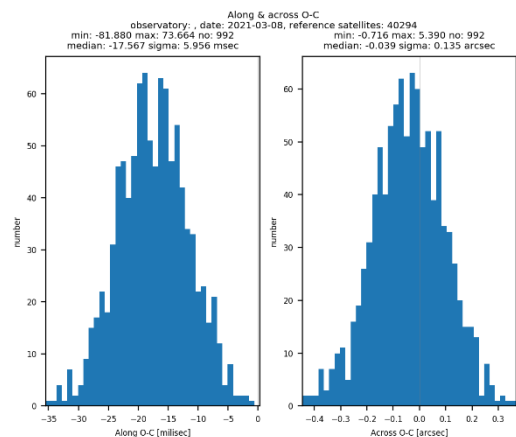


Figure 17. Distribution of errors in RA and Dec for GPS satellite observed with Andor Zyla 5.5 camera.

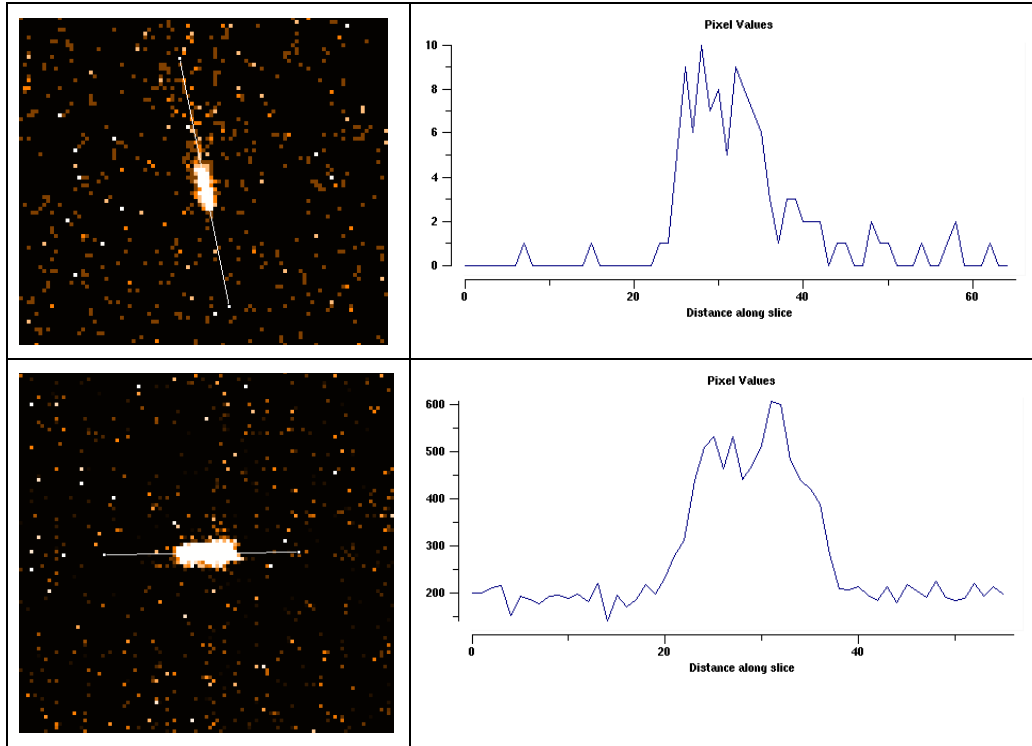


Figure 18 Top-left: Image composed of “on” events and cross-section line of star trail recorded with the DAVIS 346BSI camera. Top-right: distribution of “on” events along the cross section line. A trail of “on” events is visible to the right. Bottom: Image and cross section of star trail recorded with the Zyla camera

Overall the results for DAVIS 346BSI camera have acceptable and repeatable time bias and astrometric accuracy on par with our expectations given that Andor Zyla had significantly better limiting magnitude and more reference stars.

In order to further confirm the results of the observations, the orbital elements of the observed GPS satellite were determined using data from both cameras. The software used for this process was the GEODYN 2 package. The number of astrometric measurements with Andor Zyla was about 100 times larger than with DAVIS 346BSI camera. As all data points in GEODYN 2 have the same weights, the influence of DAVIS data points on the resulting orbit is very low. Due to this fact, the results should be interpreted only as a relative comparison of DAVIS 346BSI measurements with respect to Zyla.

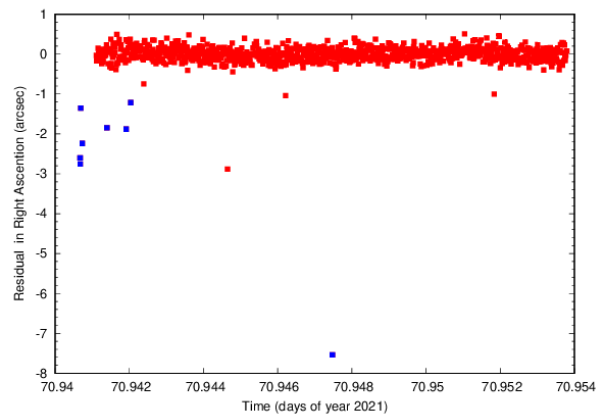


Figure 19. Orbital fit residuals in RA.

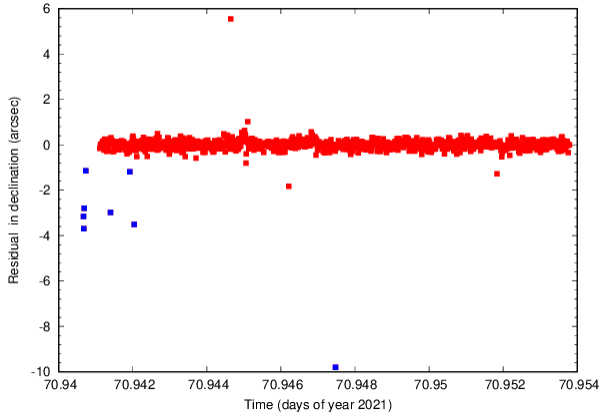


Figure 20. Orbital fit residuals in Dec

In Fig. 20 and 21, the blue dots representing the measurements from DAVIS 346BSI are deviated by a few arcsec because of its larger time bias. We can also see larger scatter because of its lower astrometric uncertainty resulting primarily from lower number of reference stars.

6.2 Ajisai satellite

Ajisai is an experimental satellite on low Earth orbit designed specifically for optical monitoring with ground-based laser stations and telescopes (NORAD - 16908, COSPAR - 1986-061A). It is a rotating sphere composed mostly of mirrors and retroreflectors. The satellite was clearly visible to the DVS during the specular reflections of sunlight.

The Ajisai satellite was observed with DAVIS 346BSI camera on a 12.5 inch f/8 telescope. With this setup, the satellite was observed 2 times in total — on the 20th of November 2020 for 120 seconds and the 13th of February 2021 for 125 seconds. The third observation of the Ajisai satellite was performed using a 12” Newton telescope and lasted 44 seconds. The event streams from the observations were converted into FITS images using 10 millisecond time steps in order to obtain high time resolution for this object. The primary objective was to determine the brightness variation period.

Aperture photometry was used for each FITS image to measure the “on” event rate. It was at the level of 0 most of the time, however during blinks of the satellite, the rate was increasing significantly. The event rate changes over the period of 2 minutes of observations are presented in Fig. 22 and the flux rate changes of “on” events are presented in Fig. 23

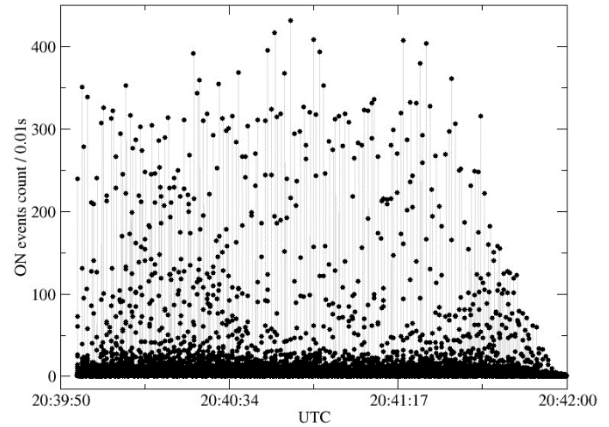


Figure 21. Event rate changes of "on" events from Ajisai satellite during 2 minutes of observation on the 20th of November 2020.

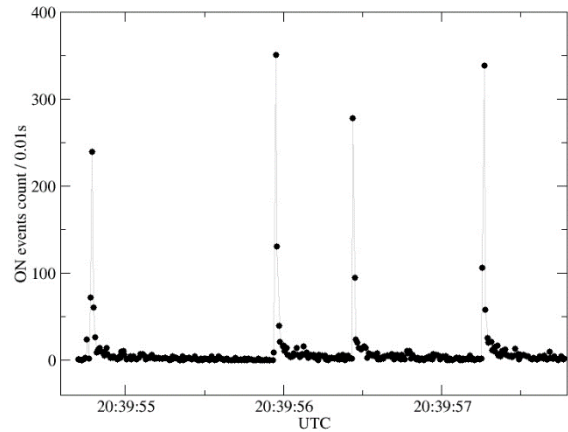


Figure 22. Flux rate changes of "on" events from Ajisai satellite during 3 seconds of observation on the 20th of November 2020.

As seen in our data, the blinks are clearly visible and they occur in a repeating pattern corresponding to the location of mirrors on the surface of the rotating satellite body. The data was analysed using Fourier periodogram with the frequency of up to 2Hz.

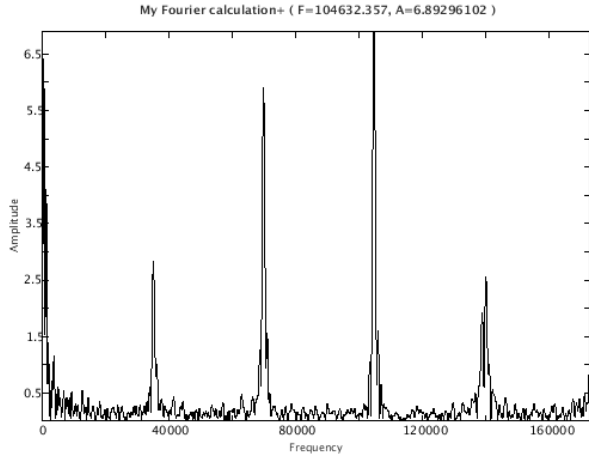


Figure 23. Fourier periodogram up to frequency of 172800 c/d (2.0 Hz) for observations on the 20th of November 2020.

The regularly distributed peaks visible in the Fig. 24 are the harmonics of the main frequency. After further inspection of event curves phased with the most prominent frequencies we decided that the actual period was $P = 34885 \pm 20.7$ c/d as it presented the lowest scatter of data points.

Similar analysis was carried out with subsequent observations. Its result is presented in Tab. 3. We also compared our determinations with long term ephemeris published in [3]. Fig. 25 shows a perfect agreement between expectation and our determination proving that DVS camera can be a valuable tool in period determination of fast rotating satellites.

UTC date	observed spin period [s]	uncertainty [s]	years after launch	ephemeris spin period [s]
2020-11-20	2.4788s	0.0014s	34.275	2.4785
2021-02-13	2.4878s	0.0019s	34.508	2.4871
2021-02-15	2.4870s	0.0021s	34.513	2.4872

Table 3. Ajsai rotation period determined.

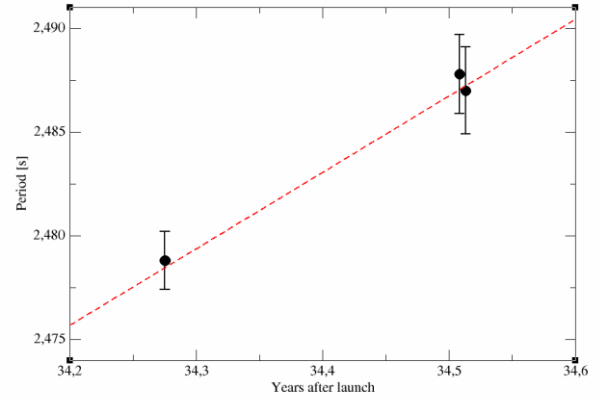


Figure 24. Three periods of the Ajsai satellite determined during this project showing a clear sign of growth, as expected from the ephemeris (dashed line) from [2].

7 CONCLUSIONS

The possibilities of present day DVS cameras, as concluded from testing the DAVIS 346BSI, in terms of ground-based observations of Earth satellites are currently limited to some extent in several areas. As opposed to modern CCD and CMOS cameras, the sizes of available detectors are very small. Currently there are not many specimens of the camera available off-the-shelf, so it is not easy to find a camera with a matching pixel size for a particular optical system. Moreover, due to the fact that the DVS cameras are not cooled, the low-light sensitivity is limited.

As a result of performing various tests on DAVIS 346BSI camera, certain prerequisites have emerged, the fulfilment of which is necessary for performing survey and tracking observations with the DVS. Firstly, the DVS camera timing has to be related to UTC time scale. It is possible through feeding the camera every few seconds with an electronic rectangular impulse generated with GNSS based clock. Thanks to this solution, the conversion of internal timestamps to UTC is possible. The second prerequisite is the conversion of the data format generated by DVS cameras (AEDAT) into FITS file format, so that it can be analysed with regular astronomical photometric or astrometric software. For this purpose, the AEDAT Converter software was developed within the project.

Once the aforementioned requirements are fulfilled, it was possible to perform several tests which shown that the limiting magnitude of the DVS proved to be worse by about 1 mag with respect to modern sCMOS sensors used at the same telescope at angular velocity $> 0.01^\circ/\text{s}$. At velocities smaller than 0.01 deg/sec the difference increases to about 3 mag. Based on the tests, the time bias of the DAVIS 346BSI camera has the value at least several milliseconds for bright targets and several dozen

milliseconds for dim targets. Moreover, the results of GNSS observations indicated that the time bias can be even larger, reaching up to about 125 milliseconds. Moreover each recorded moving target produces a “comet tail” which makes the image analysis more challenging.

It was also noted that only objects, which are brighter than about 8 mag are visible during tracking observations, while targets down to about 12.5 mag are detectable at angular velocities between $0.001^\circ/\text{s}$ and $0.01^\circ/\text{s}$. Specific software or hardware modifications can mitigate this problem, as the rotating shutter and variable telescope tracking methods provided satisfying results.

Another important finding is the fact that when the DAVIS 346BSI camera is combined with a typical astronomical telescope, astrometry is impossible in most of the cases due to lack of reference stars, which is caused mainly by the small sensor size and reduced limiting magnitude. The daytime limiting magnitude of the DAVIS 346BSI camera is about 2-3 mag, which is worse than in the case of most of the modern CMOS cameras. This makes the daytime survey or tracking observations with the DAVIS 346BSI camera (with the exception of several brightest satellites) practically impossible.

The satellite tracking is additionally straitened by the dependence of the DAVIS 346BSI camera time bias on the target brightness. In the case of this type of observations, the reference stars move in the field of view with substantial angular velocities and each of them has a different delay in DVS recording depending on its magnitude. This may cause a deformation in relative stellar positions that would have to be corrected. Therefore, when a fast-moving object is observed, an additional step in astrometric analysis is necessary for DVS sensors when compared to regular CCD or CMOS cameras. However, this effect is probably significant only in the case of tracking the fastest MEO and LEO targets.

What is worth emphasizing is the fact that the limiting magnitude of the DAVIS 346BSI camera is limited by only 1-1.5 mag with respect to modern CMOS cameras in satellite survey observations. It is possible that with the future low-noise cameras, the on-the-fly detection and analysis of objects passing in the field of view will be achievable thanks to the DVS camera low bandwidth.

The time bias in astrometric measurements of GNSS satellite performed with the DVS camera, was at the level of $\sim 125\text{ms}$ which is higher than $\sim 4\text{ms}$ reported in literature [2] and $\sim 20\text{ms}$ in our blinking LED experiments.

The overall conclusion is that the current generation of DVS cameras is a demanding tool, still at an early stage of development considering its potential astronomical use. The cameras were not developed to work under a very low light condition. Perhaps with the exception of

Ajisai satellite rotation period determination, observations with DAVIS 346BSI camera had no advantage over a CMOS camera. In order to improve DVS cameras' results and poor astrometric success rate either a much larger sensor size or much faster optical systems would be necessary. Several improvements were deemed beneficial for the DVS to be used in the future in its most promising area — satellite survey observations. Those include using fast optical systems; implementing a cooling module, thus significantly reducing the noise events generation; lowering the detection threshold from 10% to at least 3%, introducing improvements to the event stream conversion to FITS images or direct analysis of AEDAT stream and finally reducing the pixel size to match the camera properly with fast optical systems.

Regardless of the rather early stage of technological readiness of the DAVIS 346BSI camera, it is clear to see the applications where this technology is worth consideration. DVS technology might be useful in adaptive optics as a wavefront sensors camera. Another interesting prospect for the use of the DVS technology in the future is recording the lunar flashes, which are the rapid changes in the brightness of the Moon's surface caused by meteorite strikes.

Considering the presented method of DVS data stream conversion to 2D images (Fig. 26) it is obvious that we do not utilize its full survey potential. In the case of survey observations it would be beneficial to combine events into images in the direction parallel to the target's motion vector (Fig. 27). This method is equivalent to a shift-and-add (synthetic tracking) method used, among others, in very fast NEO observations. However, in contrast to the shift-and-add, with the DVS cameras it is possible to work with individual pixels and better separate them from objects and background noise. Obviously this method would have to be complemented with a searching algorithm that would identify the passage and calculate its direction.

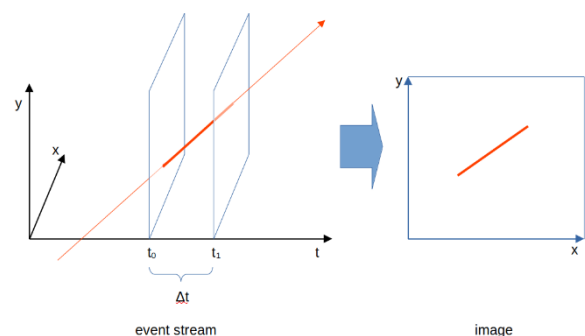


Figure 25. Standard method of converting the DAVIS event stream to a 2D image. Events are selected between two chosen moments of time and are subsequently stacked onto and XY plane parallel to the

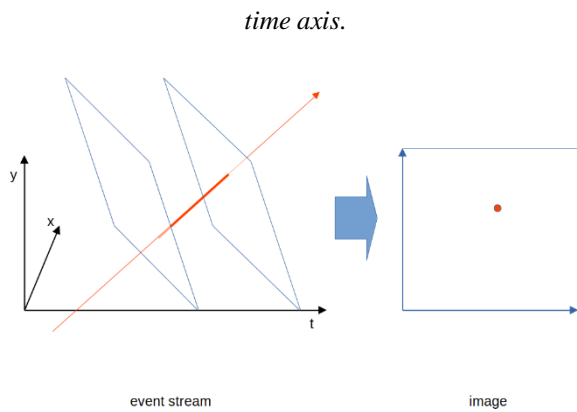


Figure 26. Adaptive event stacking in which events are combined into images along the target trail. A much higher signal to noise ratio is possible since all events corresponding to a single object are grouped together in just a few pixels.

8 REFERENCES

1. Cohen, G., Afshar, S., Schaik, A. et al (2017) "Event-based sensing for space situational awareness", *Proceedings Of The 18Th Advanced Maui Optical And Space Surveillance Technologies Conference, 19-22 September 2017*.
2. Delbruck, Hu, He (2020) "V2E: From video frames to realistic DVS event camera streams", *arXiv e-prints*.
3. Kudak V. (2017) "Studying of the own rotation period changes of satellite "Ajisai" on the interval 1986-2017", *Scientific Herald of Uzhhorod University Series Physics*.
4. Żołnowski M., Delbruck T., Kamiński K. et al. (2019) "Observational evaluation of event cameras performance in optical space surveillance", *ESA NEO SST Conference*.

